CHEMICAL ENGINEERING TRANSACTIONS
VOL. 70, 2018
A publication of AIDIC
The Italian Association of Chemical Engineering
Online at www.aidic.it/cet
Guest Editors: Timothy G. Walmsley, Petar S. Varbanov, Rongxin Su, Jiří J. Klemeš

ISBN 978-88-95608-67-9; **ISSN** 2283-9216
DOI: 10.3303/CET1870354

Study of AISI/SAE-1020 Steel Corrosion by Sulfidation from Synthetic Sulfur Compounds of Different Molecular Structures

Gerson R. Conde-Rodríguez[a,*], Javier A. Sanabria-Cala[a,b], Yuliana P. Ortíz-Patiño[a], Silvia J. Barrera-Betancur[a], Dionisio A. Laverde-Cataño[a], Dario Y. Peña-Ballesteros[a], Diego Merchan-Arenas[b]

[a]Grupo de investigaciones en corrosión, Universidad Industrial de Santander, Bucaramanga, Colombia. Parque Tecnológico Guatiguara, Km 2 vía refugio, Piedecuesta, A.A. 681011, Colombia. Tel: +57 76 344000
[b]Laboratorio de Química Orgánica Aplicada, Universidad Manuela Beltrán, Calle 33 No 26-34, Bucaramanga A.A. 678, Colombia. Fax/Tel: +57 7 6525202
conderafaelg@gmail.com

In recent years, the petrochemical industry has been affected by the decrease in global reserves of light crude oil, which has led to increase the processing of heavy crude oils with higher concentration of different contaminants that intensify corrosive phenomena. One of corrosion types that occur most frequently in the processing of heavy crude oils is sulfidation, which is caused by organic sulfur compounds of different molecular structures such as: mercaptans, sulfides, disulfides, polysulfides and thiophenes. These organic sulfur compounds are thermally decomposed at operating conditions of atmospheric distillation towers to generate hydrogen sulfide (H_2S), which reacts with the steels used in different refinery equipment, resulting in the formation of iron sulfides layers on the material surface. However, morphological properties of the iron sulfides layers formed depend on the molecular structure of the organic sulfur compounds commonly present in heavy crude oils. For this reason, in the present investigation the effect of molecular structure of different sulfur compounds on the morphological properties of corrosion products obtained by the sulfidation of AISI/SAE-1020 steel is determined. The tests are carried out using three different synthetic crude oils (SCO) prepared from a mineral oil matrix mixed with the corresponding sulfur compound: Dimethyl Sulfide, Dimethyl Disulfide and Ethanethiol. The exposure times used for the gravimetric tests were 24, 36, 48, 60 and 72 h at a constant temperature of 300 °C. Discontinuous gravimetric tests are carried out in a batch static autoclave using synthetic crude oils (SCO) with total sulfur content equal to 1 %wt. Morphological characterization of the corrosion products formed on the surface of AISI/SAE-1020 steel was carried out using the techniques Scanning Electron Microscopy (SEM), in combination with Energy-dispersive X-Ray Spectroscopy (EDS), and X-Ray Diffraction (XRD). The effect of the molecular structure of sulfur compounds on the morphological properties of iron sulfides formed on AISI/SAE-1020 steel is of great interest for the petrochemical industry due to the use of a heavy crude oil contaminant for the formation of an organic coating on the steel surface, which can inhibit corrosion by other contaminants present in the crude oil.

1. Introduction

Due to the continuous increase of world population, the energy demand has grown exponentially over the last years, reaching a value superior to 800 Mt of oil equivalent (TOE) in 2015 (International Energy Agency, 2018). Because of this high requirement, industries have needed to generate and supply large amounts of energy from traditional sources such as coal, natural gas and nuclear power plants, in addition to new sources of renewable energies such as: solar, wind power, geothermal, wave energy and biofuels, among others (Lim et al, 2009). However, crude oil remains as the most important fossil fuel, supplying about a third of the energy demand (Koch et al, 2016). Petrochemical industry is responsible for extraction, transportation, storage and refining of crude oil, processes that require the implementation of an impressive infrastructure with long sustainability over time to obtain the maximum benefit of this raw material (Sanabria et al, 2017a). However, equipment used in

Please cite this article as: Conde-Rodriguez G.R., Sanabria-Cala J.A., Ortiz-Patino Y.P., Barrera-Betancur S.J., Laverde-Catano D.A., Pena-Ballesteros D.Y., Merchan-Arenas D., 2018, Study of aisi/sae-1020 steel corrosion by sulfidation from synthetic sulfur compounds of different molecular structures , Chemical Engineering Transactions, 70, 2119-2124 DOI:10.3303/CET1870354

the processing and refining of crude oil is susceptible to damages caused by physicochemical processes during its service life, either due to operational failures or the processing of corrosive substances (Amyotte and Khan, 2016). In general, the corrosion of refinery materials is largely due to the processing of a wide variety of substances present in crude oils such as: paraffins, olefins, aromatic hydrocarbons and asphaltenes, in addition to a wide range of compounds considered contaminants such as: heavy metals, inorganic salts, amines, naphthenic acids and organic sulfur compounds, among others (Rebak, 2011). The sulfur organic compounds are the substances that promote the greatest affectation on the refining equipment, because they are the precursors of sulfidation phenomenon of the exposed materials (Jin, 2013). However, the type of molecular structure of these sulfur organic compounds has a great influence on the alloys deterioration degree and the type of corrosion products formed on the steels surface (Sharifi et al, 2017). Therefore, in the present investigation the behavior of corrosion rate by sulfidation of AISI/SAE-1020 steel was determined as a function of time and the molecular structure of sulfur organic compounds using synthetic crude oils (SCO). The present research results are of great interest for the petrochemical industry because it allows to analyze the individual effect of three different molecular structures of sulfur organic compounds, which are present mainly in heavy Colombian crude oils, allowing to advance in the understanding of corrosive phenomena that occur in ferritic materials.

2. Methodology

From an AISI/SAE-1020 steel, 50 gravimetric coupons were obtained with dimensions: 2.22 mm length, 1.22 mm width and 0.13 mm thickness. The surface preparation of each coupon was carried out using silicon carbide abrasive paper No. 150, 220, 400, 600, 1200 and 1500, to be finally cleaned in an ultrasonic bath with analytical grade acetone; subsequently, the coupons were weighed and stored in a high efficiency cabinet-type desiccator in accordance with ASTM G1-03 Standard. The material chemical composition was determined by Atomic Emission Spectrometry according to ASTM E415–17 Standard as shown in Table 1.

Table 1: Chemical composition (%wt) of AISI/SAE-1020 steel determined by Atomic Emission Spectrometry.

C	Mn	P	Si	S	Fe
0.184	0.917	0.019	0.066	<0.150	87.97

Gravimetric tests were carried out in a batch static autoclave with maximum capacity of 500 mL. Prior to the gravimetric tests, a purge with analytical nitrogen of purity 99.9 %v/v was carried out in 3 cycles of 30 minutes each to eliminate the oxygen present in the autoclave. Three synthetic crude oils (SCO) were prepared with a sulfur concentration equal to 1 %wt, using an analytical grade mineral oil as matrix and three sulfur compounds of different molecular structures and purity higher than 99.9 %a/a, which are: Dimethyl Sulfide (DMS), Dimethyl Disulfide (DMD) and Ethanethiol (ETT). The exposure times evaluated were 24, 36, 48, 60 and 72 h at a constant temperature of 300 °C. Gravimetric coupons were immersed in a volume of 200 mL of each synthetic crude oil to perform the gravimetric tests, from which the mass gain and corrosion rate of the AISI/SAE-1020 steel was calculated in accordance with the guidelines of the ASTM G1-03 Standard. Each gravimetric test was performed in triplicate to guarantee the reproducibility of the tests, calculating the respective standard deviation.

3. Results and discussion

In Figure 1, the behavior of the mass gain and the corrosion rate of AISI/SAE-1020 steel is observed, in addition to the changes that occur on material surface over time when it is exposed to the DMS synthetic crude oil. At 24 h of exposure, the appearance of a bilayer of FeS corrosion products is observed, where the internal layer presents high stability and homogeneity over the entire surface of AISI/SAE-1020 steel, while the corrosion product formed externally is darker and located in superficial random areas of the material, causing an approximate material corrosion rate of 6 mpy. However, at 36 h of exposure it is detailed that the outer layer has mostly been detached, leaving only the inner layer on the surface of the steel. This detachment is due to the increase of diffusional phenomena throughout the exposure time, generating a lower adherence of the FeS corrosion product (Ning et al, 2015). Accordingly, both the mass gain and the corrosion rate of the material exhibit a decreasing behavior. The corrosion rate of the steel at 36 h of exposure reaches an approximate value of 1 mpy, decreasing around 83 % in comparison with the value obtained at 24 h, so it is inferred that the FeS corrosion product adhered on the steel surface generated a type of protection towards the material (Sanabria et al, 2017c). In the range of 48 to 60 h of exposure is observed the formation of a new layer of FeS corrosion products on the existing internal layer, which is produced by reaction between the bisulfide ion (HS^-), generated by DMS thermal decomposition, and the iron ions from the metal matrix, which cross the layer of existing internal FeS corrosion products through diffusive phenomena (Rebak, 2011). For this reason, the mass gain increases

again and the corrosion rate for 48 and 60 h reaches approximate values of 1.2 and 2.3 mpy, respectively. However, at 72 h of exposure the mass gain of the material decreases, along with its corrosion rate, since the internal layer of FeS corrosion products promotes cycles of formation and detachment of a FeS second layer of low adherence (Hazelton et al, 2015). The FeS corrosion products formed at a temperature of 300 °C and 72 h of exposure correspond to crystalline structures of a compact hexagonal type, with clearly defined grain boundaries, approximate average grain size of 1.38 µm and a superficial sulfur content close to 9 % wt. This type of crystalline structure presents a greater surface thermodynamic stability generating homogeneous FeS corrosion products, which provide protection to the material when attack by other corrosive species present in the system (Rickard and Luther, 2007).

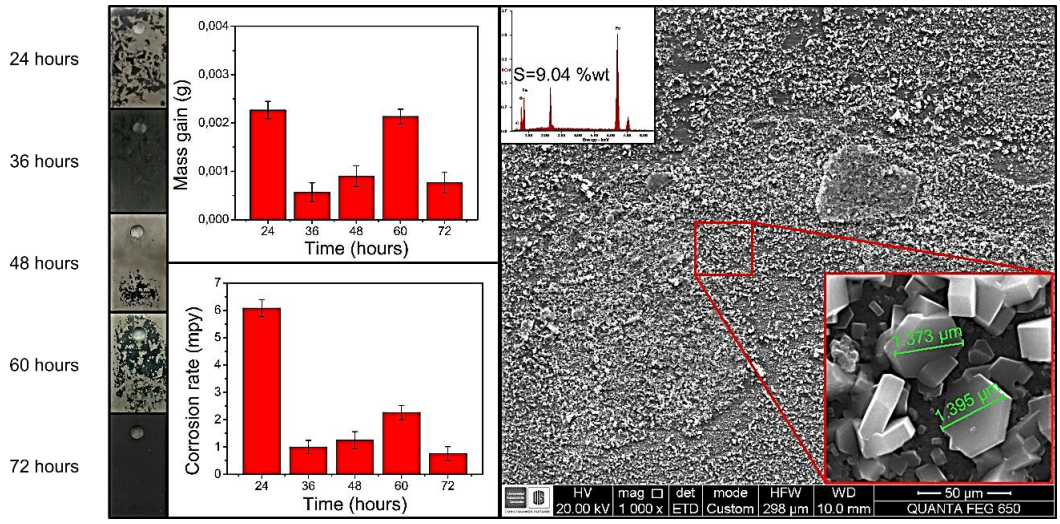

Figure 1: Mass gain, corrosion rate, photographs and SEM-EDS micrographs of the corrosion products formed on AISI/SAE-1020 steel exposed to DMS at 300°C and 72 h

In Figure 2, the behavior of mass gain and corrosion rate of the gravimetric coupons of AISI/SAE-1020 steel exposed to DMD synthetic crude oil is shown, where is evidenced the increase in mass gain and decrease in corrosion rate of AISI/SAE-1020 steel for all exposure times evaluated in the system. The behavior of the corrosion rate of AISI/SAE-1020 steel is attributed to the increase of the corrosion products thickness formed on the material surface (Sanabria et al, 2017b). However, at the steel/FeS interface it is produced the iron ions diffusion out of the metal matrix, while in the FeS/crude interface the diffusion of sulfur ions towards the material is generated, which accumulate tensile stresses on the formed layer that lead to the appearance of small cavities in the FeS corrosion products, whose coalescence causes the formation of cracks that trigger the FeS layer fracture at 72 h of exposure (William, 2015), as detailed in Figure 2. This surface phenomenon creates areas where the steel is exposed again to the synthetic crude oil, allowing the H_2S in the system to continue reacting with iron to promote the formation of an internal layer of corrosion products, which increases the mass gain through the exposure time (Ning et al, 2014). However, the mass gain slows down throughout the exposure time because the inner layer acts as a physical barrier that blocks the ions diffusion, decreasing the AISI/SAE-1020 steel corrosion rate up to 46 %, obtaining values of 25.6 mpy at 72 h of exposure. SEM results show that corrosion products formed on the material surface correspond to FeS bilayers, where the internal layer has a hexagonal crystalline structure with average grain size of 2.5 µm, while the outer layer has spinels-like crystalline monoclinic grains of with average grain size of 7.4 µm (Bai et al, 2014). From the above, it can be inferred that there is an evolution in the grain size of FeS layers, presenting smaller grains for inner layer compared with the measurements made for the outer layer, with an approximate sulfur content of 32 %wt in the analyzed surface for 72 h of exposure at 300 °C of temperature. In Figure 3, it is observed that both mass gain and corrosion rate of gravimetric coupons of AISI/SAE-1020 steel increases with respect to the exposure time when exposed to ETT synthetic crude oil. This behavior is due to the thiol bond (-SH) characteristic of ETT, which provides this sulfur compound with a high chemical reactivity, facilitating its thermal decomposition at lower exposure times and producing a greater amount of hydrogen sulfide in the system (Lepore, 2016). Thus, this compound provides a greater amount of sulfur ions in the medium to react, generating an increase in the diffusive flux of these species through the layers of corrosion products (Lepore, 2016).

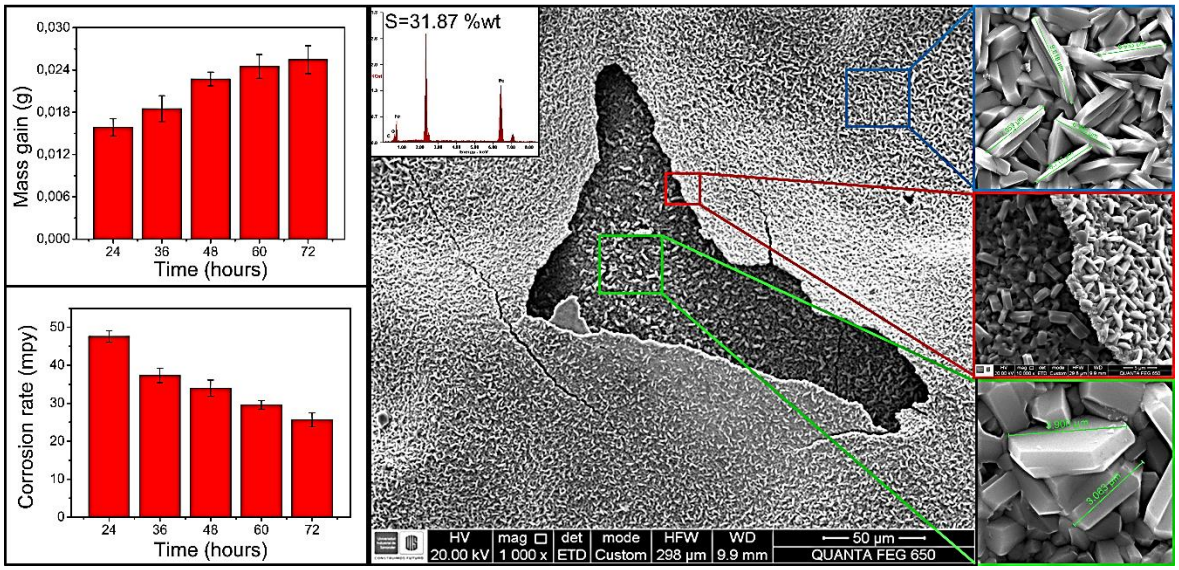

Figure 2: Mass gain, corrosion rate and SEM-EDS micrographs of the corrosion products formed on AISI/SAE-1020 steel exposed to DMD at 300°C and 72 h

The increase in the species diffusion produces an increase in the tensile stresses on the layers previously formed, which accelerates the coalescence of the cavities and allows a trilayer formation of different FeS compounds with compact hexagonal structures or non-defined crystalline structures (Shi et al, 2016), as observed in the SEM results. The layer located closer to the metal matrix has well defined grain boundaries with an average size of 1.03 µm and reached a sulfur content of 6 %wt in the analyzed area. The intermediate layer exhibits an increase in grain size and sulfur content up to 3.62 µm and 29 %wt, respectively. The outer layer has agglomerated grains with average size of 4.02 µm and sulfur content of 34.73 %wt. The first layer of corrosion products formed is fractured because the iron and sulfur ions diffuse through it to a large extent. This FeS layer grew rapidly due to the larger amount of sulfur ions available to react with the material. Because of the crack formed in the FeS layer, the metal matrix is exposed and reacts to form an intermediate layer of corrosion products, which has a lower sulfur content because the stoichiometric amount of bisulfide ion available in the system has been reduced (Jin et al, 2015). However, the diffusion of the species generates the accumulation of tensile stresses which are strong enough to produce the fracture of the intermediate layer, exposing the metallic matrix again and initiating a new chemisorption process that favors the formation of an internal layer with a lower surface content of sulfur (Xin and Dettman, 2016). The grain size of the different FeS corrosion products formed shows an increasing behavior from the internal layer to the external layer, as well as the surface content of sulfur, due to the amount of sulfur ions available during the formation process of FeS corrosion products (Jin, 2013). On the other hand, the AISI/SAE-1020 steel corrosion rate increases continuously, reaching approximate average values of 22 mpy, because the diffusion of ions does not find a homogeneous or thermodynamically stable physical barrier that blocks its diffusion, continuously deteriorating the material in the system. The analysis of the corrosion products formed at the AISI/SAE-1020 steel surface exposed to temperature of 300 °C and a time of 72 h by XRD allows the determination of the crystalline phases, which are listed in Table 2.

Table 2: Crystalline phases determined on AISI/SAE-1020 steel exposed to SCO for 72 h by XRD

Organic Sulfur Compound	Crystalline phases			
Dimethyl Sulfide (DMS)	Troilite (FeS)	Iron (Fe)	Iron sulfide (FeS)	Pyrrhotite ($Fe_{0.941}S$)
Dimethyl Disulfide (DMD)	Pyrrhotite ($Fe_{1-x}S$)	Pyrrhotite ($Fe_{0.941}S$)	Pyrrhotite ($Fe_{0.893}S$)	Pyrrhotite (Fe_7S_8)
Ethanethiol (ETT)	Iron sulfide (FeS)	Pyrrhotite ($Fe_{1-x}S$)	Pyrrhotite ($Fe_{0.941}S$)	Troilite (FeS)

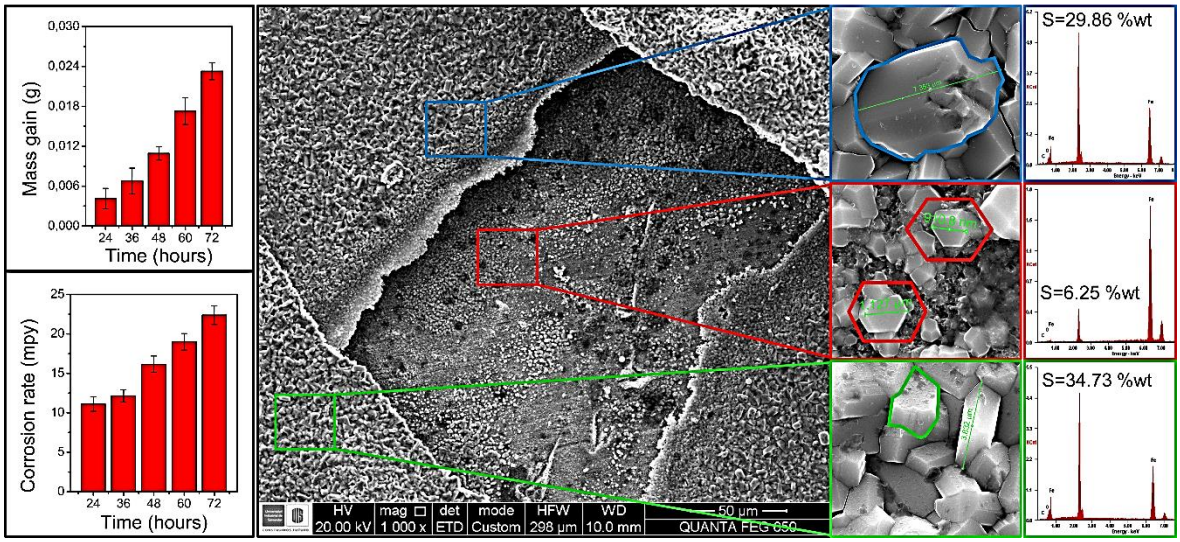

Figure 3: Mass gain, corrosion rate and SEM-EDS micrographs of the corrosion products formed on AISI/SAE-1020 steel exposed to ETT at 300°C and 72 h.

It is possible to observe that for DMS the troilite crystalline phase (FeS) is present, which is stoichiometric and has a compact hexagonal structure that allows the formation of a homogeneous layer of corrosion products (Zhang et al, 2017). On the other hand, the iron detection during the superficial characterization of the AISI/SAE-1020 steel exposed to the DMS synthetic crude oil indicates that the corrosion products layer has a low thickness, which allows the interaction of the X Ray beam with the metal matrix (Zheng et al, 2017). Otherwise, for DMD and ETT synthetic crude oils the XRD analysis allows the identification of the non-stoichiometric pyrrhotite and iron sulfide phases, which presented a lower surface thermodynamic stability and were susceptible to fractures caused by the diffusive phenomena present in the system (Huang et al, 2017).

4. Conclusions

In the present study of AISI/SAE-1020 steel corrosion by sulfidation exposed to the processing of synthetic crude oils prepared from sulfur organic compounds with different molecular structure, it can be inferred from the gravimetric tests that the sulfur compound ETT requires a lower amount of energy for thermal decomposition in the system, because it requires the breaking of a single C–S sigma bond, while DMS and DMD compounds require greater thermal energy to break two C–S sigma bonds and form hydrogen sulfide. However, when there is an H_2S excess in the system, the diffusional processes increase the tensile stresses and lead to the fracture of previously formed FeS corrosion products, exposing the metal matrix to a repeated sulfidation attack as presented for the sulfur compounds DMD and ETT, which generated FeS corrosion products such as non-stoichiometric pyrrhotite and iron sulfide with non-defined grain boundaries. On the other hand, the DMS synthetic crude oil generates troilite corrosion products, which have crystalline structures of a compact hexagonal type and present a greater homogeneity and thermodynamic stability on the AISI/SAE-1020 steel surface, isolating the material and reducing the sulfidic corrosion rate of the material up to 87 %.

Acknowledgments

The authors want to thank Grupo de Investigaciones en Corrosión (GIC) – UIS and Laboratorio de Química Orgánica Aplicada (LQOA) from Universidad Manuela Beltrán for research funding of this project.

References

Amyotte P., Khan F., 2016, What do gas blows, iron dust accumulations and sulfidation corrosion have in common? Chemical Engineering Transactions, 48, 739–744, DOI:10.3303/CET1648124

ASTM International, Standard E415–17, 2011, Standard test method for analysis of carbon and low-alloy steel by Spark Atomic Emission Spectrometry, West Conshohocken, USA.

ASTM International, Standard G1–03, 2011, Standard practice for preparing, cleaning, and evaluating corrosion test specimens, West Conshohocken, USA.

Bai P., Zheng S., Zhao H., Ding Y., Wu J., Chen C., 2014, Investigations of the diverse corrosion products on steel in a hydrogen sulfide environment, Corrosion Science, 87, 397–406.

Hazelton M., Stephenson T., Lepore J., Subramani V., Mitlin D., 2015, Sulfide promoted chronic fouling in a refinery: Broad phenomenon spanning a range of heat transfer surfaces and oil types, Fuel, 160, 479–489.

Huang F., Cheng P., Dong Y., Liu J., Hu Q., Zhao X., Cheng Y., 2017, Characterization of surface films formed during corrosion of a pipeline steel in H_2S environments, Journal of Materials Engineering and Performance, 26, 2, 828–836.

International Energy Agency, 2018, IEA HEADLINE GLOBAL ENERGY DATA (2017 edition), <iea.org/statistics> accessed 12.01.2018

Jin P., 2013, Mechanism of corrosion by naphthenic acids and organosulfur compounds at high temperatures, PhD Thesis, Ohio University, Ohio, USA.

Jin P., Nesic S., Wolf H., 2015, Analysis of corrosion scales formed on steel at high temperatures in hydrocarbons containing model naphthenic acids and sulfur compounds, Surface and Interface Analysis, 47, 454–465.

Koch G., Varney J., Thompson N., Moghissi O., Gould M., Payer J., 2016, International Measures of Prevention, Application, and Economics of Corrosion Technologies Study – IMPACT, NACE International, Houston, Texas, USA.

Lepore J., 2016, The role of sulfur species in establishing the corrosion reactions in refinery metallurgies, MSc Thesis, University of Alberta, Alberta, Canada.

Lim W., Kim J., Park S., Moon I., 2009, The development of corrosion control document (ccd) in refinery: crude distillation unit process, Chemical Engineering Transactions, 17, 1419–1424, DOI:10.3303/CET0917237

Ning J., Zheng Y., Brown B. Young D., Nesic S., 2015, A thermodynamic model for the prediction of mild steel corrosion products in an aqueous hydrogen sulfide environment, Corrosion, 71, 8, 945–960.

Ning J., Zheng Y., Young D., Brown B., Nesic S., 2014, Thermodynamic study of hydrogen sulfide corrosion of mild steel, Corrosion, 70, 4, 375–389.

Rebak R., 2011, Sulfidic corrosion in refineries – A review, Corrosion Reviews, 29, 123–133.

Rickard D., Luther G., 2007, Chemistry of iron sulfides, Chemical Reviews, 107, 514–562.

Sanabria J., Laverde D., Peña D., Merchan D., 2017a, Influence of temperature and time on the corrosion by sulfidation of AISI-316 steel exposed under transfer line, Chemical Engineering Transactions, 57, 715–720, DOI: 10.3303/CET1757120

Sanabria J., Mejía C., Laverde D., Peña D., Sarmiento H., 2017b, Role of corrosion products by the sulfidation of AISI/SAE-1020 steel in heavy crude oil at high temperatures, Chemical Engineering Transactions, 57, 1435–1440, DOI: 10.3303/CET1757240

Sanabria J., Montañez N., Laverde D., Peña D., Mejía C., 2017c, Evaluation of corrosion products formed by sulfidation as inhibitors of the naphthenic corrosion of AISI-316 steel, Journal of Physics: Conference Series, 935, No. 012051.

Sharifi S., Liang A., Cooke D., Chapman D., Chaloner B., Kuperman A., 2017, High-temperature sulfidic corrosion of carbon steel in model oil/sulfur compound blends, Corrosion Conference & Expo, No. 8909.

Shi F., Zhang L., Yang J., Lu M., Ding J., Li H., 2016, Polymorphous FeS corrosion products of pipeline steel under highly sour conditions, Corrosion Science, 102, 103–113.

William F., 2015, Mechanisms governing the growth, reactivity and stability of iron sulfides, PhD Thesis, Massachusetts Institute of Technology, Cambridge, USA.

Xin Q., Dettman H., 2016, Corrosivity study of sulfur compounds and naphthenic acids under refinery conditions, Corrosion, No. 7392.

Zhang L., Li H., Shi F., Yang J., Hu L., Lu M., 2017, Environmental boundary and formation mechanism of different types of H_2S corrosion products on pipeline steel, International Journal of Minerals, Metallurgy and Materials, 24, 4, 401–409.

Zheng Y., Ning J., Brown B., Young D., Nesic S., 2015, Mechanistic study of the effect of iron sulfide layers on hydrogen sulfide corrosion of carbon steel, Corrosion, No. 5933.